Multi-angle Beam Steering for Head-Mounted Displays

Daming Xu, Guanjun Tan, Shin-Tson Wu
College of Optics and Photonics, University of Central Florida, Orlando, FL 32816, USA

Abstract
We propose a switchable multi-angle grating for steering the light between nine different angles from 0° to 16° with an interval of 2°. It shows great promises for eye-tracking applications in head-mounted displays.

Author Keywords
Liquid crystal, diffraction grating, head-mounted displays

1. Introduction

Head-mounted display (HMD) [1-3] is an emerging technology with widespread applications in entertainment, military training, education, and medical diagnostics, etc. A fully developed HMD usually provides a visual coupling system such as head/eye tracker that slaves head/eye positions and motions to a dynamic viewpoint in a virtual environment. Thus, a key challenge of these HMDs is to track eye movement and display images accordingly [4-5]. A simple approach is to steer the displayed images to human eye dynamically. The eye tracker detects the movement of human eye so that the exit pupil is adjusted accordingly to accommodate positioning error. So far, the eye tracking technology has been investigated extensively; but how to adjust the exit pupil continuously to ensure the light can be perceived by human eye remains a challenge.

A feasible solution is to use liquid crystal (LC) grating. The liquid crystal technology has become indispensable not only in displays [6-8] but also in tunable photonic devices [9-11] due to its low cost, lightweight, and low power consumption. However, most of LC gratings exhibit slow response time (~10-100ms) [12-15] and low diffraction efficiency (≤ 26%) [16-18], which would induce lag in rendering and degrade optical efficiency. Recently, extensive efforts have been devoted to solve these problems. In particular, tunable phase gratings using polymer-stabilized blue phase liquid crystal (PSBPLC) showing submillisecond response time and high diffraction efficiency have been demonstrated [19-20]. But the major tradeoffs are twofold: high driving voltage (~150V) and noticeable hysteresis [21]. Meanwhile, the PS-BPLC require special fabrication conditions, such as temperature control and UV polymerization [22-23].

On the other hand, most LC phase gratings possess a small diffraction angle (~3°), which originates from the large grating constant. Since the fabrication of small-dimension electrodes is very challenging, there is limited room to enlarge the diffraction angle. Moreover, for the LC gratings investigated so far, their structural periodicity is fixed once fabrication is completed. Therefore, the diffraction angles cannot be tuned electronically.

In this paper, we demonstrate a high-efficiency and large-angle phase grating using a fringe field switching (FFS) liquid crystal cell. The FFS phase grating can diffract >32% light to the 2nd orders with a diffraction angle of 12.1°. And it possesses a high contrast ratio as well as fast response time. Based on this operation principle, we design a multi-angle beam steering device to steer light between 0° and 16° with an interval of 2°.

2. Fringe Field Switching Grating

The LC director distribution of an FFS LC grating at voltage-off and -on states are depicted in Figs. 1(a) and 1(b), respectively. At V = 0, a tiny diffraction results from the index mismatch between ITO electrodes and LC, as Fig. 1(c) shows. Although higher orders can be observed, their intensity is negligible as compared to that of the 0th order since the ITO layer is very thin. The grating constant is $\Lambda_1 = (W + L)$. As the applied voltage increases, the LC directors are reoriented gradually along the electric field [24-25]. The LC directors are vertically aligned on top of the grid electrodes and at the center between the electrodes, as shown in Fig. 1(b). Hence, the periodic phase distribution appears, which functions as a diffraction grating. Since the phase difference is symmetric w.r.t. the center the electrode gap, the grating constant is reduced to $\Lambda_2 = \Lambda_1/2$. Consequently, the diffraction angle is doubled compared to the voltage-off state, thus achieving a large-angle grating, as shown in Fig. 1(d).

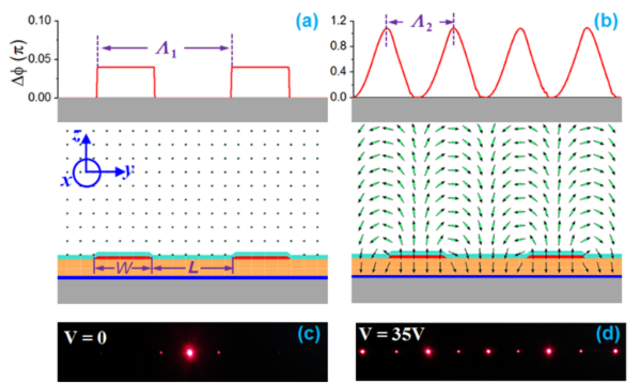

Figure 1. LC distribution, phase profile and diffraction patterns of an FFS cell at (a, c) V = 0 and (b, d) V= 35V.

Figure 2(a) shows the experimental setup for measuring the diffraction efficiency. The polarizer is used to select the TM-polarized light. An iris was placed behind the FFS cell to select the diffraction order. The dots in Fig. 2(b) represent the measured diffraction efficiency of the 0th to 4th orders. As the applied voltage increases, the energy is transferred from the 0th to ±2nd order at an angle of 12.1°. The diffraction efficiency is the same for the +2 and −2 orders, both can achieve 32.1% at 70V with a contrast ratio over 800:1. The measured data agree well with the numerical model we developed [26]. Since diffraction efficiency gradually saturates in the high voltage region, if we are willing to sacrifice 2% in diffraction efficiency, then we can obtain 30% diffraction efficiency at 35V. In addition, we measured the polarization of the 2nd order and found the output light is elliptically polarized with an aspect ratio of 25.6:1, which can be regarded as almost linear.

In addition, we also measured the response time of the 2nd diffraction orders. The rise time is 0.21ms and decay time 2.95ms at 23°C; both of which are much faster than those of

 ISSN 0097-966X/16/4703-1826-$1.00

nematic LC gratings (typically ~10-100ms). More attractively, due to the ultralow viscosity and low activation energy of our LC material UCF-L1 [27], even if the temperature drops to –40°C the decay time is still as fast as 40.4 ms. Hence, our phase grating remains functional for low-temperature outdoor HMD applications.

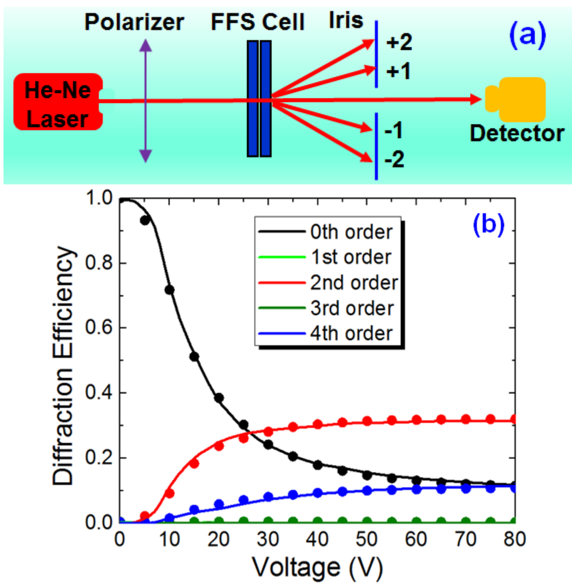

Figure 2. (a) Experimental setup for measuring diffraction efficiency. (b) Measured data (dots) and simulation results (solid curves).

3. Blazed Phase Grating

Based on the FFS grating, we propose a blazed phase grating that can be freely switched between different angles using a fringe in-plane switching (FIS) cell [28]. The device configuration is depicted in Fig. 3(a). The basic structure of the FIS cell remains the same as the FFS cell but the pixel electrodes are not necessarily in the same potential: adjacent pixel electrodes are applied with V_1 and V_2 voltages, respectively. To steer the light to ±2nd orders, same voltage is applied to the adjacent pixels ($V_1 = V_2 > 0$) and the device operates in the same principle as the FFS cell, as Fig. 3(b) illustrates. In order to steer the light to ±1st orders, we keep $V_1 \neq V_2$ so that not only a fringe field is formed between pixel and common electrodes but also an in-plane electric field is generated between pixel electrodes. Therefore, the grating constant is enlarged to $\Lambda = (W + L)$ again and most light are diffracted to ±1st orders [Fig. 3(c)].

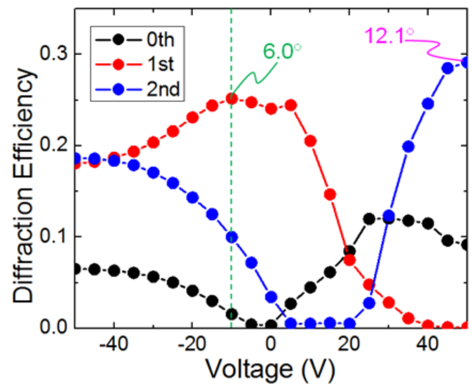

Figure 4. Simulated diffraction efficiency of 0th, 1st and 2nd orders when V_2 is scanned from –50V to 50V (V_1 is fixed at 50V).

Figure 4 depicts the simulated voltage-dependent diffraction efficiency of 0th, 1st and 2nd orders for this blazed grating. To reveal the energy transfer between different orders, V_1 is fixed at 50V and V_2 is scanned from –50V to 50V. From Fig. 4, when V_2 = –10V, the 1st order can achieve 26.4% efficiency at a diffraction angle θ_1 = 5.9° whereas diffraction efficiency of the 2nd order is much lower, only 9.7%. As V_2 increases, more energy starts to transfer from 1st order back to 0th order. As V_2 exceeds 0V, energy starts to transfer to 2nd order since the electric field between adjacent pixel electrodes becomes weaker and the symmetric LC director distribution w.r.t. the center of electrode gap starts to build up. When V_2 reaches the same potential as V_1, the device functions in the same way as the FFS cell, thus directing the light onto the 2nd order with a diffraction efficiency of 29.4% at the diffraction angle θ_2=12.1°. Thus, our blazed grating can switch between three orders flexibly. Nevertheless, it may still not be able to meet the requirement of the adjusting the exit pupil in a wide range of angles for the HMDs. Therefore, we propose two cascaded switchable blazed

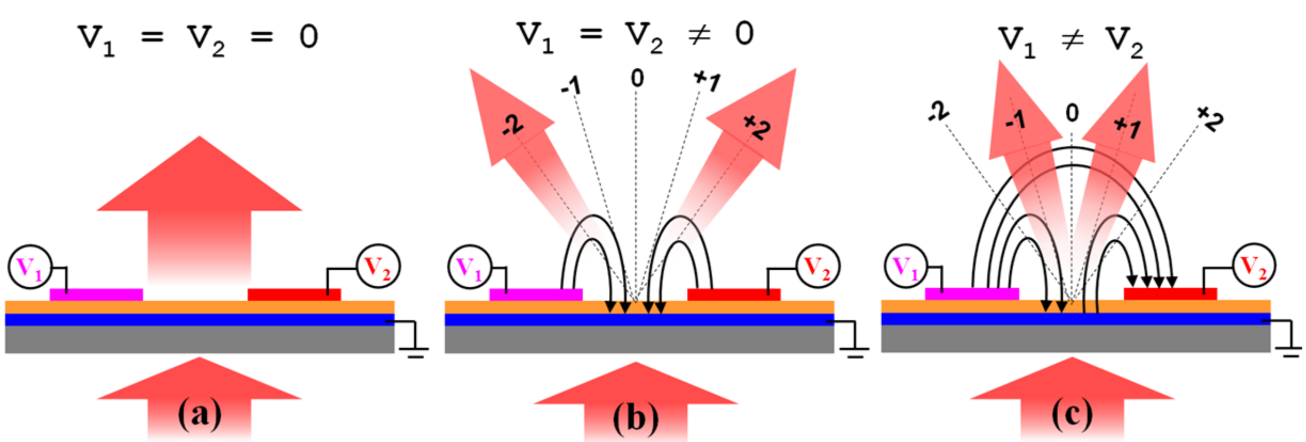

Figure 3. Physical principles of the blazed grating using a FIS LC cell under different voltage conditions.

gratings to achieve multi-directional beam steering, as will be discussed below.

4. Cascaded Switchable Gratings

The blazed grating is able to switch light between 0^{th}, 1^{st} and 2^{nd} orders, but for eye tracking in HMDs we need multiple diffraction angles. In this case, cascaded gratings can be considered.

4.1 Static cascaded mode

In the static cascade mode, two blazed gratings with different electrode dimensions are stacked together, as shown in Fig. 5. The electrode width and gap in the 1^{st} blazed grating are different from those in the 2^{nd} blazed grating. Here, we set W_1 = 3μm and L_1 = 4μm, same as the FFS cell mentioned above. Hence, the first blazed grating is able to steer the incident light from 0° to 6.0° and 12.1°. In order to steer the light to direction between the diffraction orders of the first blaze grating, the dimension of the second blazed grating can be set larger. For instance, if we set W_2 = 4μm and L_1 = 5.3μm, the 2^{nd} blazed grating will be able to steer light to 4.5° and 9.0°. Consequently, by operating two blazed gratings independently, we are able to steer light discreetly between 0° and 12.1° with five different angles (0°, 4.5°, 6.0°, 9.0° and 12.1°).

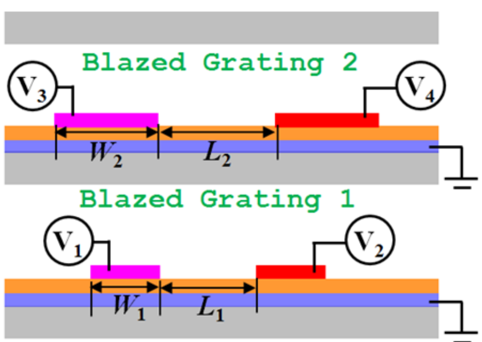

Figure 5. Device configuration of a cascaded grating.

4.2 Dynamic cascaded mode

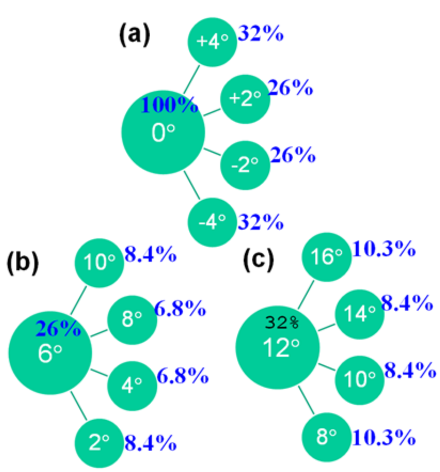

Figure 6. The cascade between different diffraction orders of two gratings.

In addition to static mode, the cascaded gratings can also be operated under dynamic mode. As mentioned above, the measured aspect ratio of the outgoing light is 25.6:1, which can be approximated as a linearly polarized light. Thus, if two gratings are operated simultaneously so that the output light of the first blazed grating is used as the input light of the second blazed grating. For example, when we set the dimension of the 2^{nd} blazed grating to be three times larger than the first grating so that the 2^{nd} grating is able to steer light to 2° and 4°, as shown in Fig. 6(a). When the 1^{st} order output light (~26%) of the first blazed grating transmits through the 2^{nd} grating, the light would be diffracted to 10°, 8°, 4° and 2°, as shown in Fig. 6(b). Similarly, when the 2^{nd} order output light (~32%) of the first blazed grating transmits through the 2^{nd} grating, the light would be diffracted to 16°, 14°, 10° and 8° with a different diffraction efficiency, as shown in Fig. 6(c). By simple arithmetic, all the diffraction angles can be determined. Thus, we are able to steer the light between 0° and 16° with an interval of 2°.

5. Conclusion

We have experimentally demonstrated a high-efficiency (>32%) and large-angle (12.1°) FFS LC grating. It possesses a relatively fast response time, even at -40°C. Based on this, we proposed to cascade two FFS gratings to steer a beam between 0° and 16° with an interval of 2°. It exhibits great promises for eye-tracking applications in head-mounted displays.

6. Acknowledgments

The authors are indebted to Dr. Ming-Chun Lee of AU Optronics (Taiwan) for providing the FFS cells, Dr. Xiaolong Song of HCCH (China) for providing a liquid crystal mixture HAI- 653265, and AFOSR for partial financial support under contract No. FA9550-14-1-0279.

7. References

[1] O. Cakmakci, J. Rolland, "Head-worn displays: a review," J. Disp. Technol. **2**, 199 (2006).
[2] B. Furht, Handbook of Augmented Reality (Springer, 2011).
[3] R. A. Earnshaw, Virtual reality systems (Academic press, 2014).
[4] V. Tanriverdi, R. J. Jacob, "Interacting with eye movements in virtual environments," CHI Lett. 2(1), 265 (2000).
[5] A. T. Duchowski, V. Shivashankaraiah, T. Rawls, et al. "Binocular eye tracking in virtual reality for inspection training," Proc. Symp. Eye Tracking, 89 (2000).
[6] E. Lueder, Liquid Crystal Displays: Addressing Schemes and Electro-Optical Effects (Wiley, 2001).
[7] Z. Luo, D. Xu, S. T. Wu, "Emerging quantum-dots-enhanced LCDs," J. Disp. Technol. **10**, 526 (2014).
[8] D. Franklin, Y. Chen, A. Vazquez-Guardado, S. Modak, et al. "Polarization-independent actively tunable color generation on imprinted plasmonic surfaces," Nature Commun. **6**, 7337 (2015).
[9] Y. H. Lin, H. S. Chen, H. C. Lin, Y. S. Tsou, et al. "Polarizer-free and fast response microlens arrays using polymer-stabilized blue phase liquid crystals," Appl. Phys. Lett. **96**, 113505 (2010).
[10] M. Xu, D. Xu, H. Ren, I. S. Yoo, Q. H. Wang, "An adaptive liquid lens with radial interdigitated electrode," J. Opt. **16**, 105601 (2014).
[11] F. Peng, D. Xu, H. Chen, S. T. Wu, "Low voltage polymer network liquid crystal for infrared spatial light modulators," Opt. Express **23**, 2361 (2015).
[12] R. G. Lindquist, J. H. Kulick, G. P. Nordin, et al. "High resolution liquid-crystal phase grating formed by fringing fields from interdigitated electrodes," Opt. Lett. **19**, 670 (1994).
[13] D. Subacius, P. J. Bos, O. D. Lavrentovich, "Switchable diffractive cholesteric gratings," Appl. Phys. Lett. **71**, 1350 (1997).

[14] I. Drevensek-Olenik, M. Copic, M. E. Sousa, G. P. Crawford, "Optical retardation of in-plane switched polymer dispersed liquid crystals," J. Appl. Phys. **100**, 033515 (2006).
[15] J. Chen, P. J. Bos, H. Vithana, D. L. Johnson, "An electrooptically controlled liquid-crystal diffraction grating," Appl. Phys. Lett. **67**, 2588 (1995).
[16] S. M. Morris, D. J. Gardiner, F. Castles, P. J. W. Hands, T. D. Wilkinson, H. J. Coles, "Fast-switching phase gratings using in-plane addressed short-pitch polymer stabilized chiral nematic liquid crystals," Appl. Phys. Lett. **99**, 253502 (2011).
[17] F. Fan, A. K. Srivastava, V. G. Chigrinov, and H. S. Kwok, "Switchable liquid crystal grating with sub millisecond response," Appl. Phys. Lett. **100**, 111105 (2012).
[18] A. K. Srivastava, W. Hu, V. G. Chigrinov, A. D. Kiselev, Y. Q. Lu, "Fast switchable grating based on orthogonal photo alignments of ferroelectric liquid crystals," Appl. Phys. Lett. **101**, 031112 (2012).
[19] J. Yan, Y. Li, S. T. Wu, "High-efficiency and fast-response tunable phase grating using a blue phase liquid crystal," Opt. Lett. **36**, 1404 (2011).
[20] G. Zhu, J. N. Li, X. W. Lin, H. F. Wang, et al. "Polarization independent blue-phase liquid-crystal gratings driven by vertical electric field," J. Soc. Inf. Disp. **20**, 341(2012).
[21] D. Xu, J. Yan, J. Yuan, F. Peng, Y. Chen, and S. T. Wu, "Electro-optic response of polymer-stabilized blue phase liquid crystals," Appl. Phys. Lett. 105(1), 011119 (2014).
[22] Y. Liu, S. Xu, D. Xu, J. Yan, Y. Gao, S. T. Wu, "A hysteresis-free polymer-stabilised blue-phase liquid crystal," Liq. Cryst. **41**, 1339 (2014).
[23] D. Xu, J. Yuan, M. Schadt, S. T. Wu, "Blue phase liquid crystals stabilized by linear photo-polymerization," Appl. Phys. Lett. **105**, 081114 (2014).
[24] S. H. Lee, S. L. Lee, H. Y. Kim, "Electro-optic characteristics and switching principle of a nematic liquid crystal cell controlled by fringe-field switching," Appl. Phys. Lett. **73**, 2881 (1998).
[25] D. Xu, F. Peng, H. Chen, J. Yuan, S. T. Wu, M. C. Li, S. L. Lee, W. C. Tsai, "Image sticking in liquid crystal displays with lateral electric fields," J. Appl. Phys. **116**, 193102 (2014).
[26] D. Xu, G. Tan, S. T. Wu, "Large-angle and high-efficiency tunable phase grating using fringe field switching liquid crystal," Opt. Express **23**, 12274 (2015).
[27] H. Chen, F. Peng, Z. Luo, D. Xu, S. T. Wu, M. C. Li, S. L. Lee, W. C. Tsai, "High performance liquid crystal displays with a low dielectric constant material," Opt. Mater. Express **4**, 2262 (2014).
[28] J. W. Park, Y. J. Ahn, J. H. Jung, S. H. Lee, R. Lu, H. Y. Kim, S. T. Wu, "Liquid crystal display using combined fringe and in-plane electric fields," Appl. Phys. Lett. **93**, 081103 (2008).